Stimulus Specificity of Gene Expression Programs Determined by Temporal Control of IKK Activity

Shannon L. Werner *et al.*

Science **309**, 1857 (2005);
DOI: 10.1126/science.1113319

Nature often builds on a single mechanism to increase specificity and complexity. For transcription, increasingly complex genomes often contain a greater number of transcription factor family members than separate transcription factor families (*26*). This suggests that diversity within a gene family may provide specificity and versatility. Here the canonical pathway of NF-κB activation, which is activated once in cells treated with TNFα, is activated twice in response to TLR4 stimulation to create a distinct NF-κB activation profile.

References and Notes

1. S. Ghosh, M. J. May, E. B. Kopp, *Annu. Rev. Immunol.* **16**, 225 (1998).
2. A. S. Baldwin, *J. Clin. Invest.* **107**, 241 (2001).
3. E. Pikarsky *et al.*, *Nature* **431**, 461 (2004).
4. T. Bouwmeester *et al.*, *Nat. Cell Biol.* **6**, 97 (2004).
5. K. H. Cho, S. Y. Shin, H. W. Lee, O. Wolkenhauer, *Genome Res.* **13**, 2413 (2003).
6. A. Hoffmann, A. Levchenko, M. L. Scott, D. Baltimore, *Science* **298**, 1241 (2002).
7. D. E. Nelson *et al.*, *Science* **306**, 704 (2004).
8. M. S. Hayden, S. Ghosh, *Genes Dev.* **18**, 2195 (2004).
9. K. Brown, S. Park, T. Kanno, G. Franzoso, U. Siebenlist, *Proc. Natl. Acad. Sci. U.S.A.* **90**, 2532 (1993).
10. M. L. Scott, T. Fujita, H. C. Liou, G. P. Nolan, D. Baltimore, *Genes Dev.* **7**, 1266 (1993).
11. S. C. Sun, P. A. Ganchi, D. W. Ballard, W. C. Greene, *Science* **259**, 1912 (1993).
12. K. Kawasaki, H. Nogawa, M. Nishijima, *J. Immunol.* **170**, 413 (2003).
13. G. M. Barton, R. Medzhitov, *Science* **300**, 1524 (2003).
14. S. Akira, K. Takeda, T. Kaisho, *Nat. Immunol.* **2**, 675 (2001).
15. E. Meylan *et al.*, *Nat. Immunol.* **5**, 503 (2004).
16. M. Yamamoto *et al.*, *Science* **301**, 640 (2003).
17. M. Yamamoto *et al.*, *Nat. Immunol.* **4**, 1144 (2003).
18. Materials and methods are available as supporting material on *Science* Online.
19. J. A. DiDonato, M. Hayakawa, D. M. Rothwarf, E. Zandi, M. Karin, *Nature* **388**, 548 (1997).
20. F. Mercurio *et al.*, *Science* **278**, 860 (1997).
21. S. Doyle *et al.*, *Immunity* **17**, 251 (2002).
22. T. H. Leung, A. Hoffmann, D. Baltimore, *Cell* **118**, 453 (2004).
23. Z. Jiang, T. W. Mak, G. Sen, X. Li, *Proc. Natl. Acad. Sci. U.S.A.* **101**, 3533 (2004).
24. S. Sato *et al.*, *J. Immunol.* **171**, 4304 (2003).
25. J. Gohda, T. Matsumura, J. Inoue, *J. Immunol.* **173**, 2913 (2004).
26. E. S. Lander *et al.*, *Nature* **409**, 860 (2001).
27. D. E. Seborg, T. F. Edgar, D. A. Mellichamp, *Process Dynamics and Control, Wiley Series in Chemical Engineering* (John Wiley & Sons, New York, 1989), pp. 7–130.

28. We thank M. Yamamoto and S. Akira for generously providing the MEFs; M. Boldin, M. Meffert, and A. Hoffmann for valuable discussions; and the Millard and Muriel Jacobs Genetics and Genomics Laboratory at the California Institute of Technology for assistance with the gene expression study. This work was funded by the NIH (GM039458-21). M.W.C. is a Robert Black Fellow supported by the Damon Runyon Cancer Research Foundation (DRG-#1835-04). T.H.L. is a student in the UCLA–California Institute of Technology Medical Scientist Training Program and supported by the Achievement Rewards for College Scientists foundation.

Supporting Online Material

www.sciencemag.org/cgi/content/full/309/5742/1854/DC1
Materials and Methods
Fig. S1
Tables S1 and S2
References

15 March 2005; accepted 28 July 2005
10.1126/science.1112304

Stimulus Specificity of Gene Expression Programs Determined by Temporal Control of IKK Activity

Shannon L. Werner,* Derren Barken,* Alexander Hoffmann†

A small number of mammalian signaling pathways mediate a myriad of distinct physiological responses to diverse cellular stimuli. Temporal control of the signaling module that contains IκB kinase (IKK), its substrate inhibitor of NF-κB (IκB), and the key inflammatory transcription factor NF-κB can allow for selective gene activation. We have demonstrated that different inflammatory stimuli induce distinct IKK profiles, and we examined the underlying molecular mechanisms. Although tumor necrosis factor–α (TNFα)–induced IKK activity was rapidly attenuated by negative feedback, lipopolysaccharide (LPS) signaling and LPS-specific gene expression programs were dependent on a cytokine-mediated positive feedback mechanism. Thus, the distinct biological responses to LPS and TNFα depend on signaling pathway–specific mechanisms that regulate the temporal profile of IKK activity.

The evolutionarily conserved, signal-responsive transcription factor NF-κB plays a role in a myriad of physiological functions. These include lymphoid tissue development, immune, inflammatory, and environmental stress responses, and neuronal signaling (*1*, *2*). A number of human pathologies are caused by the impairment of signal-responsive NF-κB regulation, including chronic inflammatory diseases (*3*) and cancers (*4*). Thus, mechanisms that regulate NF-κB activity and allow it to control stimulus-specific physiological responses are of pressing clinical relevance (*5*, *6*) and are also of interest as a model system for studies of complex mammalian signaling systems.

NF-κB is held in an inactive state by association with one of three IκB proteins. In response to stimulation, the IκB kinase (IKK) phosphorylates NF-κB-bound IκB proteins, targeting them for proteolysis through the ubiquitin-proteasome pathway (*7*). A mathematical model based on ordinary differential equations recapitulated signaling of the IKK-IκB-NF-κB signaling module in response to the inflammatory cytokine tumor necrosis factor–α (TNFα) in murine embryonic fibroblasts (MEFs) (*8*). This model predicted dynamic signaling behavior resulting from IκB resynthesis, as observed biochemically (*8*) or in single-cell real-time imaging studies (*9*). Further refinements of the model have led to correct predictions of cross-regulation between IκB family members (*10*) and have uncovered important negative feedback mediated by the IκBε isoform (*11*).

The functional pleiotropism of NF-κB is based on the responsiveness of IKK to diverse signals transduced by plasma membrane–bound receptors or subcellular organelles (Fig. 1A) (*12*). Although different stimuli activate the same IKK-IκB-NF-κB signaling module, they elicit different gene expression programs. Because temporal control of NF-κB activity can lead to selective gene expression (*8*), we reasoned that stimulus-specific temporal control of IKK activity might allow for distinct biological responses if signal processing within the IKK-IκB-NF-κB signaling module resulted in distinct NF-κB activity profiles. To examine the signal processing characteristics of the signaling module, we generated a collection of potential IKK profiles with a simple algorithm (Fig. 1B). The algorithm allows for variable rises in IKK activity (over a time period of a = 0, 60, 120, or 240 min), a first plateau of various amplitudes (x = 4, 12, 34, or 101 nM) and durations (b = 0, 5, 15, 30, 60, or 120 min), variable decays (over a time period of c = 0, 60, 120, or 240 min), and a second, equal or lower, plateau of activity at or above baseline (y = 1, 4, 12, 34, or 101 nM).

The resulting comprehensive library of 687 distinct IKK activity profiles (fig. S1) served as inputs for computational simulations with our newly refined mathematical model (*13*). Each IKK input-NF-κB output pair (examples in Fig. 1C) reflects signal processing within the IKK-IκB-NF-κB signaling module. By grouping similar NF-κB activity profiles using standard K-means clustering, we investigated which IKK activity profiles are distinguished

Signaling Systems Laboratory, Department of Chemistry and Biochemistry, 9500 Gilman Drive, Mailcode 0375, La Jolla, CA 92093–0375, USA.

*These authors contributed equally to this work.
†To whom correspondence should be addressed. E-mail: ahoffmann@ucsd.edu

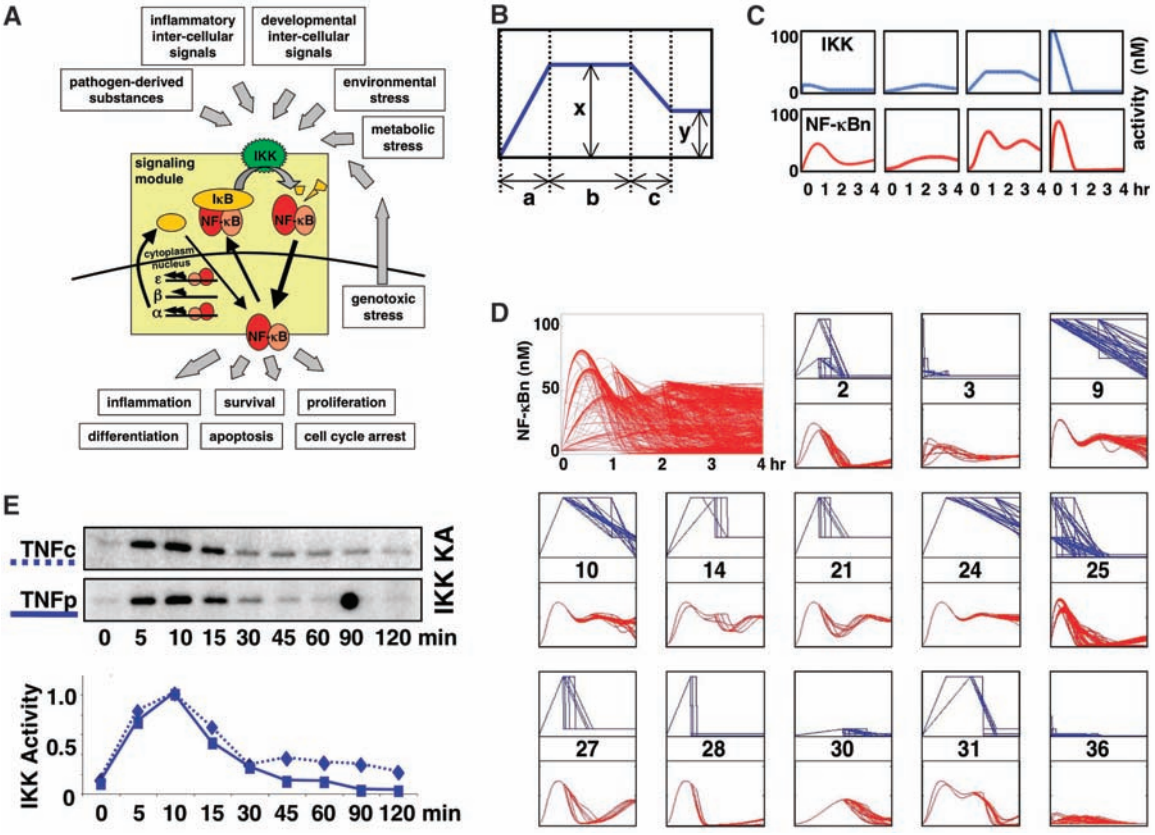

Fig. 1. Exploring the temporal control of IKK activity in regulating NF-κB signaling. (**A**) The schematic illustrates that many physiological signals impinge on the IKK-IκB-NF-κB signaling module to produce different physiological responses. (**B**) A set of diverse IKK profiles was computationally generated by the following algorithm: Each input had a rising phase (parameter *a*), a first plateau (parameter *b*), a falling phase (parameter *c*), and a second plateau, each with varying time values of 0, 60, 120, or 240 min (parameter *a*), or 0, 5, 15, 30, 60, or 120 min (parameter *b*), or 0, 60, 120, or 240 min (parameter *c*). The heights of the first (parameter *x*) and second (parameter *y*) plateaus were also varied to 4, 12, 34, or 101 nM IKK (parameter *x*), or 1, 4 12, 34, or 101 nM IKK (parameter *y*) ($y \leq x$). (**C**) Four examples from a library of 687 distinct IKK activity profiles (blue) that were generated as described in (**B**). The resulting NF-κB activity profile (red) was computed using the mathematical model of the IKK-IκB-NF-κB signaling module, version 2.0 (*13*). (**D**) NF-κB activity profiles (red, top left) produced by 687 IKK profiles were clustered by K-means clustering (MatLab 7.0 Statistical Toolbox). Shown here is a selection of 13 out of 36 clusters (for all, see fig. S2). The corresponding IKK profiles (blue) were grouped accordingly. (**E**) IKK activity was measured in mouse embryonic fibroblasts (MEFs) after chronic (TNFc) or 45-min pulse (TNFp) TNF stimulation (1 ng/ml) by IKK IP-kinase assay (IKK KA). GST-IκBα(1-54) served as a substrate in the assay, and its phosphorylation by IKK was quantitated, normalized, and graphed.

by the signaling module and which profiles, although seemingly different, are likely to have similar biological effects. Examination of the clusters (Fig. 1D and fig. S2) revealed, for example, that the amplitude of the first peak of IKK activity was not a major determinant of the NF-κB activity profile (for example, clusters 2 and 25). However, different rates of IKK activation (contrast clusters 9 and 10) and the duration of the first peak of activity (contrast clusters 14 and 21, or 28 and 31) did result in different NF-κB activity profiles. The signaling module does not distinguish very much between different decay rates of IKK activity at late times (for example, clusters 9 and 24). However, the level of IKK activity in the second phase (secondary plateau) was very important (compare clusters 21, 27, and 28). Although transient aberrations in IKK activity do not result in much NF-κB activity (cluster 36), large but very transient IKK activities have similar signaling effects as sustained smaller increases (cluster 3): Both result in an NF-κB activity profile that persists much longer than the duration of the transient pulse of IKK activity. The signaling module appears to be particularly sensitive to sustained low IKK activity (cluster 30) but robust to transient perturbations.

One prediction of this computational exploration was that long-lasting NF-κB activity may be mediated by unexpectedly low amplitudes of IKK activity, whereas transient NF-κB activity requires a much higher increase in IKK activity. Examining the actual kinase activity profiles in cells exposed to either brief (45 min) or prolonged stimulation with TNFα revealed that IKK was highly active at early time points but that activity dropped to low levels after about 30 min (Fig. 1E). Consistent with the computational investigation, IKK activity profiles were similar, with only a slightly increased late plateau of activity elicited by persistent stimulation. However, these stimulation conditions have distinct biological effects mediated by a late phase of NF-κB activity (*8*). The importance of small changes in late or prolonged IKK activity suggests that mechanisms may have evolved to modulate it with remarkable precision.

Actual cellular IKK activity profiles are determined by signaling pathways emanating from receptors that allow for stimulus-specific signal processing (fig. S3). We therefore measured the IKK activity profiles in response to the inflammatory stimuli TNF and bacterial lipopolysaccharide (LPS), which engage TNF receptor TNFR and toll-like receptor 4 (TLR4), respectively. Transient administration of these stimuli (45 min) resulted in different IKK activity profiles (Fig. 2A and fig. S4). LPS elicited a small increase in IKK activity within the first 30 min, a larger increase between 45 and 90 min, and a slowly attenuating late phase. In contrast, TNF elicited a sharp peak of IKK activity within the first 15 min, with a return to baseline within 60 min. Computational simulations with those experimentally determined IKK activity profiles predicted temporally distinct NF-κB activity profiles (Fig. 2B). Experimental analysis revealed temporal NF-κB activity profiles (Fig. 2C) and IκB protein levels (fig. S5) similar to those predicted. Thus, our computational model recapitulates NF-κB activation events in response to multiple inflammatory stimuli. The successful in silico reconstitution of LPS and TNF signaling may mean that no further biochemical factors and mechanisms need be invoked to explain the regulation of nuclear NF-κB translocation by IKK.

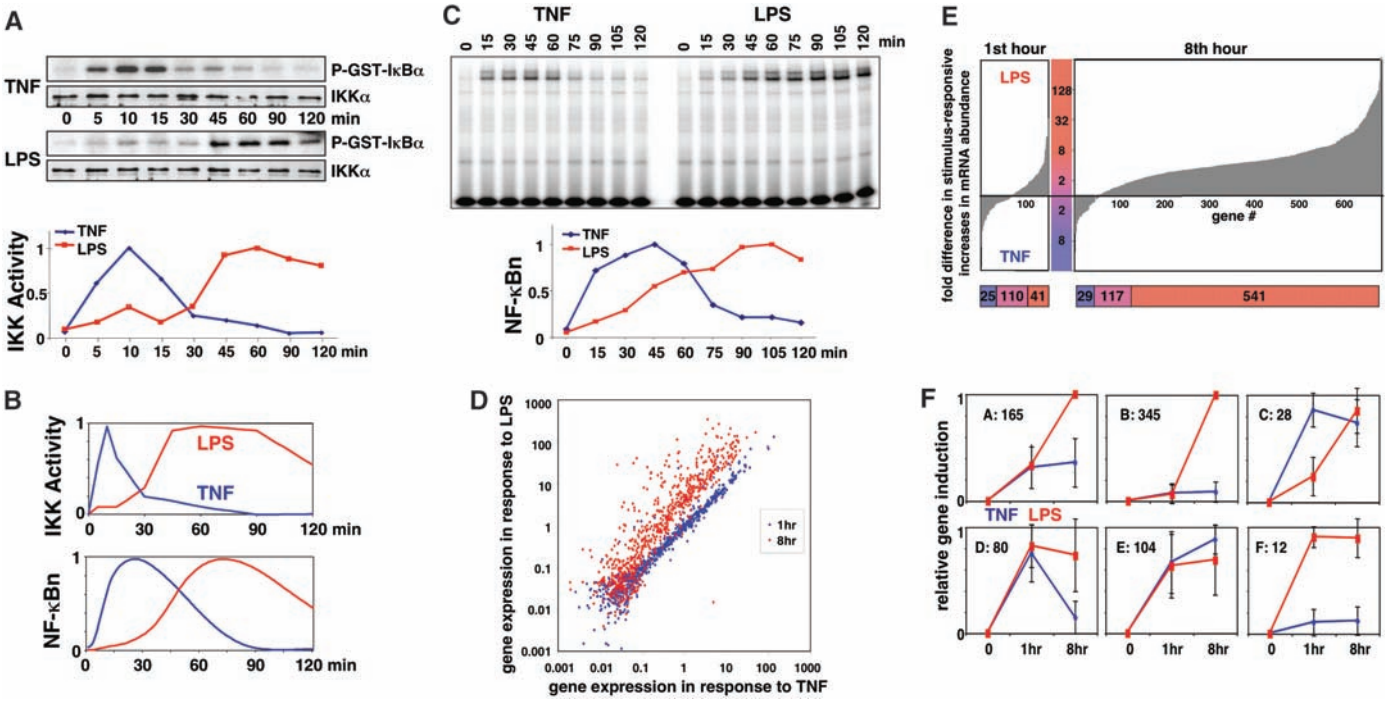

Fig. 2. Stimulus-specific signaling by the IKK-NF-κB signaling module. (**A**) IKK profiles were measured by IKK IP-kinase assay in MEFs stimulated with a 45-min pulse of either TNF (1 ng/ml) or LPS (0.1 μg/ml). Equal protein loading was confirmed with an immunoblot against IKKα. Quantitated and normalized results were graphed. (**B**) IKK profiles measured in (A) were graphed on a linear time scale (top) and used as inputs in computational simulations to predict normalized NF-κB activity profiles (bottom) in response to TNF (blue) or LPS (red). (**C**) NF-κB activity profiles were measured by electrophoretic mobility shift assay (EMSA) in response to a 45-min pulse TNF (1 ng/ml) and LPS (0.1 μg/ml). Results from the EMSA were normalized and graphed. (**D**) Microarray gene expression profiling revealed 734 genes whose expression was increased by a factor of >3 in response to either LPS or TNF stimulation at the 1- or 8-hour time point. mRNA transcript levels of each gene (in arbitrary units) are shown for the 1-hour (blue) and 8-hour (red) time points after TNF stimulation (*x* axis) and LPS-stimulation (*y* axis). (**E**) Of the genes shown in (D), 176 showed increased expression by a factor >3 in response to either LPS or TNF in hour 1 and 687 genes in hour 8. For each gene, the relative difference in the induction fold in response to TNF and LPS was calculated and graphed after ordering the genes from high TNF specificity (left) to high LPS specificity (right). The Venn diagram (bottom) details the number of genes whose expression is preferentially increased (by a factor of >2) in response to TNF (blue) or LPS (red) stimulation. Genes that do not show stimulus specificity are represented by the violet box. (**F**) Genes whose expression is increased by a factor of >3 in response to either TNF or LPS (734 total) were grouped by clustering of their normalized induction folds at time points 1 and 8 hours. The mean, standard deviation, and number of genes present in a selected number of clusters are indicated.

We used gene expression microarrays to compare gene expression programs in response to transient stimulation of MEFs with LPS and TNF. Although there was substantial overlap between LPS- and TNF-induced gene expression programs at early time points, many genes showed higher transcript levels at late times in response to LPS than to TNF (Fig. 2D). Indeed, of the genes whose expression was induced by a factor of >3 by either TNF or LPS at 1 hour, only a minority were stimulus specific (66/176 = 37.5%), whereas a majority were more highly induced by LPS at the 8-hour time point (541/687 = 78.7%) (Fig. 2E). Temporal clustering of the normalized fold-induction data of responding genes (Fig. 2F) confirmed that small numbers of genes are either coregulated by TNF and LPS (cluster E, 104 members) or are stimulus specific at the early time point (clusters C and F, 40 members). Interestingly, a very large number of genes are expressed in a LPS-specific manner at the late time point (clusters A, B, and D, 590 members). LPS-specific late gene activation correlates with the LPS-specific secondary plateau of IKK activity.

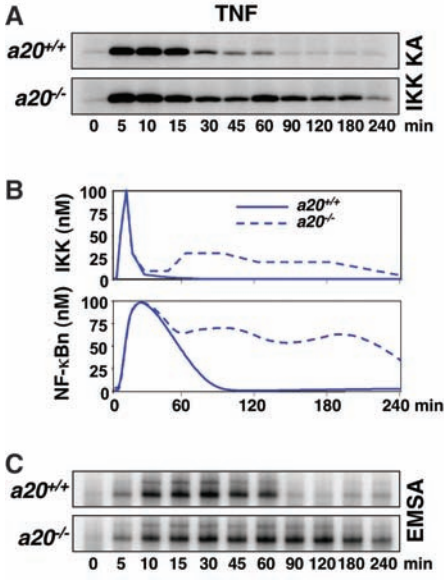

Fig. 3. Temporal control of TNF signaling through A20-mediated negative feedback. (**A**) IKK activity profiles were measured by IKK IP-kinase assays from $a20^{+/+}$ and $a20^{-/-}$ cells in response to 45-min pulse TNF stimulation over a 4-hour time course. (**B**) Quantitated experimental IKK data (top) was used as an input for computational simulations that predicted NF-κB activity profiles in $a20^{+/+}$ and $a20^{-/-}$ cells (bottom). (**C**) NF-κB activity profiles were measured by EMSA in response to 45-min pulse TNF in $a20^{+/+}$ and $a20^{-/-}$ cells over a 4-hour time course.

These observations emphasize the potential importance of late IKK activity, whose regulation may be subject to stimulus-responsive protein synthesis.

In the TNFR signaling pathway, the NF-κB response gene *A20* has been proposed to function in postinduction attenuation of NF-κB activity by modulating the signaling

mechanisms that regulate IKK activation (*14*, *15*). Using our computational model, we examined whether misregulation of IKK in A20-deficient cells was sufficient to explain the increased activation of NF-κB and the consequent inflammatory phenotype seen in A20-deficient mice. Quantitative measurements of the TNF-induced IKK activity profile in wild-type and *a20*$^{-/-}$ cells (Fig. 3A) were used as inputs of our computational model to predict NF-κB activation profiles (Fig. 3B). Biochemical analyses of nuclear NF-κB activity (Fig. 3C) and cytoplasmic IκB protein levels (fig. S6) match the computational predictions. Thus, A20 appears to function in fibroblasts in attenuating NF-κB signaling by modulating the temporal profile of IKK activity in the TNF signaling pathway but less so in the LPS signaling pathway (fig. S7).

For the TLR4 signaling pathway, the molecular mechanisms that regulate IKK are less well understood (*16*). LPS-induced IKK activity has a biphasic profile (Fig. 2B and fig. S3). By using the ribosome inhibitor cycloheximide, we found that the LPS-specific second phase of IKK activity was dependent on new protein synthesis (Fig. 4A) and varied with the density of the primary cells in culture (Fig. 4B). Consequently, we hypothesized that LPS-specific primary response genes may function to potentiate late IKK activity through an autocrine mechanism. LPS rapidly increased expression of genes encoding 10 secreted cytokines and chemokines, many of which were also expressed in response to TNF stimulation (Fig. 4C). However, the interleukin-10 (IL-10),

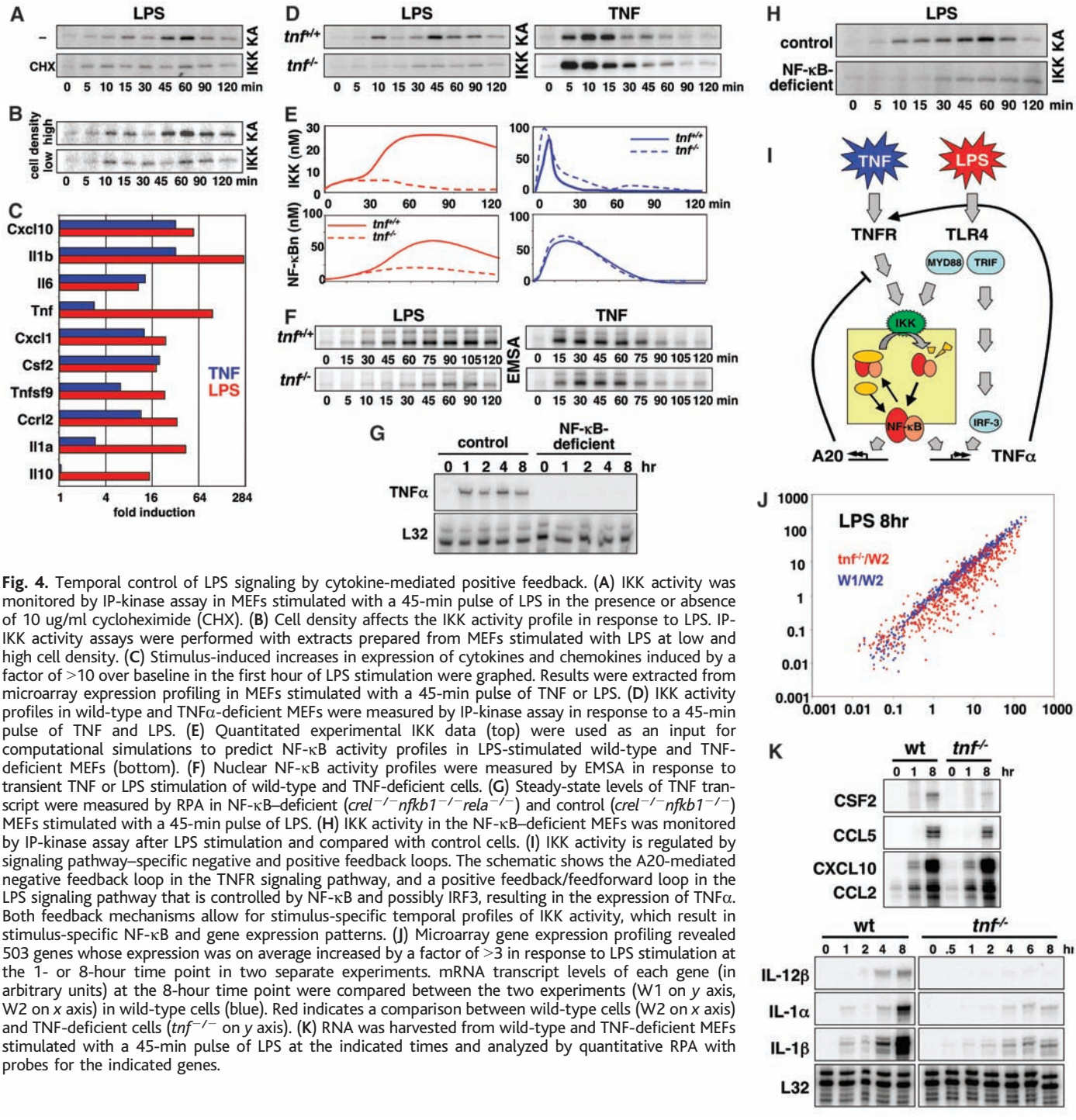

Fig. 4. Temporal control of LPS signaling by cytokine-mediated positive feedback. (**A**) IKK activity was monitored by IP-kinase assay in MEFs stimulated with a 45-min pulse of LPS in the presence or absence of 10 ug/ml cycloheximide (CHX). (**B**) Cell density affects the IKK activity profile in response to LPS. IP-IKK activity assays were performed with extracts prepared from MEFs stimulated with LPS at low and high cell density. (**C**) Stimulus-induced increases in expression of cytokines and chemokines induced by a factor of >10 over baseline in the first hour of LPS stimulation were graphed. Results were extracted from microarray expression profiling in MEFs stimulated with a 45-min pulse of TNF or LPS. (**D**) IKK activity profiles in wild-type and TNFα-deficient MEFs were measured by IP-kinase assay in response to a 45-min pulse of TNF and LPS. (**E**) Quantitated experimental IKK data (top) were used as an input for computational simulations to predict NF-κB activity profiles in LPS-stimulated wild-type and TNF-deficient MEFs (bottom). (**F**) Nuclear NF-κB activity profiles were measured by EMSA in response to transient TNF or LPS stimulation of wild-type and TNF-deficient cells. (**G**) Steady-state levels of TNF transcript were measured by RPA in NF-κB–deficient (*crel*$^{-/-}$*nfkb1*$^{-/-}$*rela*$^{-/-}$) and control (*crel*$^{-/-}$*nfkb1*$^{-/-}$) MEFs stimulated with a 45-min pulse of LPS. (**H**) IKK activity in the NF-κB–deficient MEFs was monitored by IP-kinase assay after LPS stimulation and compared with control cells. (**I**) IKK activity is regulated by signaling pathway–specific negative and positive feedback loops. The schematic shows the A20-mediated negative feedback loop in the TNFR signaling pathway, and a positive feedback/feedforward loop in the LPS signaling pathway that is controlled by NF-κB and possibly IRF3, resulting in the expression of TNFα. Both feedback mechanisms allow for stimulus-specific temporal profiles of IKK activity, which result in stimulus-specific NF-κB and gene expression patterns. (**J**) Microarray gene expression profiling revealed 503 genes whose expression was on average increased by a factor of >3 in response to LPS stimulation at the 1- or 8-hour time point in two separate experiments. mRNA transcript levels of each gene (in arbitrary units) at the 8-hour time point were compared between the two experiments (W1 on *y* axis, W2 on *x* axis) in wild-type cells (blue). Red indicates a comparison between wild-type cells (W2 on *x* axis) and TNF-deficient cells (*tnf*$^{-/-}$ on *y* axis). (**K**) RNA was harvested from wild-type and TNF-deficient MEFs stimulated with a 45-min pulse of LPS at the indicated times and analyzed by quantitative RPA with probes for the indicated genes.

IL-1α, IL-1β, and TNF genes were specifically expressed in response to LPS. TNF functions in endotoxin toxicity by a proinflammatory paracrine mechanism (*17*, *18*). When we stimulated TNF-deficient cells at high density with LPS, the late phase of IKK activity was lost, whereas TNFR-responsive IKK activation remained intact (Fig. 4D). With these measured IKK profiles, our computational model predicted a defect in NF-κB activation by LPS in TNF-deficient cells (Fig. 4E), which we confirmed experimentally (Fig. 4F).

By employing MEFs deficient in canonical NF-κB proteins, we revealed that LPS-induced expression of TNF requires NF-κB (Fig. 4G). Furthermore, LPS-induced IKK activity was lower in NF-κB–deficient cells than in controls (Fig. 4H), whereas TNF-induced IKK activity was largely unaffected by NF-κB deficiency (fig. S8). Together, these results indicate that TNF involvement in TLR4 signaling constitutes a positive feedback mechanism. TLR4 signaling to IKK was previously shown to be mediated by the adaptor protein MyD88 and, with delayed kinetics, by TRIF through an unknown signaling pathway (*16*, *19*). Our data suggest that the proposed signaling pathway is mediated by de novo synthesis of TNF (Fig. 4I). Secondary IKK activation mediated by TNF autocrine feedback may thus depend not only on the first phase of NF-κB activity, as shown here, but also possibly on TRIF-dependent IRF-3 activity.

To address whether this LPS-specific IKK regulatory mechanism determines LPS-specific gene expression, we examined gene expression in TNF-deficient cells. At the 1-hour time point, gene expression profiles overlapped with controls (fig. S9), but at the 8-hour time point, a large group of genes showed lower expression in $tnf^{-/-}$ cells than in controls (Fig. 4J). Specifically, and as confirmed by RNase protection assays (RPA) (Fig. 4K and fig. S10), late expression of colony-stimulating factor 2 (CSF2), IL-12β, IL-1α, and IL-1β was dependent on TNF, but late expression of chemokine (C-C motif) ligand 5 (CCL5), CCL2, and chemokine (C-X-C motif) ligand 10 (CXCL10) was not.

These findings indicate that TNF (and possibly other cytokines) mediate feedforward mechanisms in response to endotoxin challenges that produce positive feedback on IKK activity (and likely also regulate other signal transduction events) and are critical for the induction of a stimulus-specific gene expression program. The particular sensitivity of the biological response to the temporal profile of IKK activity suggests that the underlying molecular mechanisms [including negative and positive feedback mechanisms (Fig. 4I)] may provide sensitive signaling nodes that cells may use for signaling cross-talk.

References and Notes

1. S. Gerondakis, M. Grossmann, Y. Nakamura, T. Pohl, R. Grumont, *Oncogene* **18**, 6888 (1999).
2. S. Ghosh, M. Karin, *Cell* **109** (suppl), S81 (2002).
3. Y. Yamamoto, R. B. Gaynor, *J. Clin. Invest.* **107**, 135 (2001).
4. B. B. Aggarwal, *Cancer Cell* **6**, 203 (2004).
5. M. Karin, Y. Yamamoto, Q. M. Wang, *Nat. Rev. Drug Discov.* **3**, 17 (2004).
6. J. E. Darnell Jr., *Nat. Rev. Cancer* **2**, 740 (2002).
7. S. Ghosh, M. J. May, E. B. Kopp, *Annu. Rev. Immunol.* **16**, 225 (1998).
8. A. Hoffmann, A. Levchenko, M. L. Scott, D. Baltimore, *Science* **298**, 1241 (2002).
9. D. E. Nelson *et al.*, *Science* **306**, 704 (2004).
10. R. Quiambao *et al.*, in preparation.
11. J. D. Kearns, S. Basak, S. L. Werner, C. S. Huang, A. Hoffmann, in preparation.
12. H. L. Pahl, *Oncogene* **18**, 6853 (1999).
13. Materials and Methods are available as supporting material on *Science* Online.
14. E. G. Lee *et al.*, *Science* **289**, 2350 (2000).
15. I. E. Wertz *et al.*, *Nature* **430**, 694 (2004).
16. S. Akira, K. Takeda, T. Kaisho, *Nat. Immunol.* **2**, 675 (2001).
17. B. Beutler, V. Kruys, *J. Cardiovasc. Pharmacol.* **25** (suppl 2), S1 (1995).
18. B. Beutler, I. W. Milsark, A. C. Cerami, *Science* **229**, 869 (1985).
19. G. M. Barton, R. Medzhitov, *Science* **300**, 1524 (2003).

20. We thank C. Huang for excellent technical assistance; A. Ma for A20-deficient 3T3 cells; T. Huxford for GST-IκBα(1-54); Santa-Cruz Biotechnology for antibodies; and A. Levchenko, G. Ghosh, S. Subramaniam, and D. Baltimore for insightful discussions. This study was supported by NIH grants GM72024 and GM071573.

Supporting Online Material

www.sciencemag.org/cgi/content/full/309/5742/1857/DC1
Materials and Methods
Figs. S1 to S10
Tables S1 to S7
References

8 April 2005; accepted 28 July 2005
10.1126/science.1113319

HST2 Mediates *SIR2*-Independent Life-Span Extension by Calorie Restriction

Dudley W. Lamming,[1]* Magda Latorre-Esteves,[1]* Oliver Medvedik,[1]* Stacy N. Wong,[2]* Felicia A. Tsang,[2] Chen Wang,[2] Su-Ju Lin,[2]† David A. Sinclair[1]†

Calorie restriction (CR) extends the life span of numerous species, from yeast to rodents. Yeast Sir2 is a nicotinamide adenine dinucleotide (NAD^+)–dependent histone deacetylase that has been proposed to mediate the effects of CR. However, this hypothesis has been challenged by the observation that CR can extend yeast life span in the absence of Sir2. Here, we show that Sir2-independent life-span extension is mediated by Hst2, a Sir2 homolog that promotes the stability of repetitive ribosomal DNA, the same mechanism by which Sir2 extends life span. These findings demonstrate that the maintenance of DNA stability is critical for yeast life-span extension by CR and suggest that, in higher organisms, multiple members of the Sir2 family may regulate life span in response to diet.

A major cause of aging in the yeast *Saccharomyces cerevisiae* stems from homologous recombination between ribosomal DNA (rDNA) repeat sequences and the formation of extrachromosomal circles of rDNA known as ERCs, which accumulate exponentially and eventually lead to the death of the mother cell (*1*, *2*). The Fob1 protein promotes ERC formation by stalling rDNA replication forks, which are inherently unstable structures (*3*). Accordingly, deletion of *FOB1* reduces ERC formation and extends yeast life span (*4*).

In contrast, ERC formation is repressed by the activity of Sir2, an NAD^+-dependent histone deacetylase (HDAC) that catalyzes the formation of heterochromatin at the rDNA locus (*5*–*8*) and is the founding member of the sirtuin deacetylase family. Additional copies of the *SIR2* gene extend yeast life span by decreasing ERC formation, whereas deletion of *SIR2* increases ERC formation and shortens life span (*9*), a phenotype that can be suppressed by deleting *FOB1* (*4*).

The life span of most species including *S. cerevisiae* is extended by CR (*10*). Yeast and *Drosophila* lacking the *SIR2* gene do not live longer when subjected to CR, suggesting that Sir2 underlies this life-span extension (*11*–*15*). However, there is increasing evidence that the situation is not so simple (*16*–*18*). Although CR is blocked by a *sir2*Δ mutation, CR can extend the life span of yeast cells lacking both *SIR2* and *FOB1* (*18*, *19*). CR can also extend the life span of *Caenorhabditis elegans* worms

[1]Paul F. Glenn Laboratories for the Biological Mechanisms of Aging, Department of Pathology, Harvard Medical School, 77 Avenue Louis Pasteur, Boston, MA 02115, USA. [2]Center for Genetics and Development, and Section of Microbiology, University of California Davis, 351 Briggs Hall, Davis, CA 95616, USA.

*These authors contributed equally to this work.
†To whom correspondence should be addressed. E-mail: slin@ucdavis.edu (S.-J.L.), david_sinclair@hms.harvard.edu (D.A.S.)